1 **A systematic analysis of diet-induced nephroprotection reveals overlapping and**

2 **conserved changes in cysteine catabolism**

3

4 **Authors:** Felix C. Koehler[1,2,3], Chun-Yu Fu[4], Martin R. Späth[1,2], K. Johanna R. Hoyer-Allo[1,2],

5 Katrin Bohl[1,2,3], Heike Göbel[5], Jan-Wilm Lackmann[2], Franziska Grundmann[1], Thomas

6 Osterholt[1], Claas Gloistein[1], Joachim D. Steiner[1,6], Adam Antebi[6], Thomas Benzing[1,2,3],

7 Bernhard Schermer[1,2,3], Günter Schwarz[3,4*], Volker Burst[1] and Roman-Ulrich Müller[1,2,3*]

8

9 **Affiliations:**

10 [1] Department II of Internal Medicine, University of Cologne, Faculty of Medicine and

11 University Hospital Cologne; Cologne, 50937, Germany

12 [2] CECAD, University of Cologne, Faculty of Medicine and University Hospital Cologne;

13 Cologne, 50931, Germany

14 [3] Center for Molecular Medicine Cologne, University of Cologne; Cologne, 50931, Germany

15 [4] Institute of Biochemistry, Faculty of Mathematics and Natural Sciences, University of

16 Cologne; Cologne, 50931, Germany

17 [5] Institute for Pathology, Diagnostic and Experimental Nephropathology Unit, Faculty of

18 Medicine and University Hospital Cologne; Cologne, 50937, Germany

19 [6] Max Planck Institute for Biology of Ageing; Cologne, 50931 Germany

20

21 ***Corresponding authors**:

22 Roman-Ulrich Müller, MD

23 Department II of Internal Medicine and Center for Molecular Medicine Cologne, University

24 of Cologne, Faculty of Medicine and University Hospital Cologne; Cologne, 50937,

25 Germany

26   Tel.: +49 221 478 30966; E-mail: roman-ulrich.mueller@uk-koeln.de

27

28   Günter Schwarz, PhD

29   Institute of Biochemistry, Faculty of Mathematics and Natural Sciences, University of

30   Cologne; Cologne, 50931, Germany

31   Tel.: +49 221 470 6441; E-mail: gschwarz@uni-koeln.de

Abstract:

Caloric Restriction (CR) extends lifespan and augments cellular stress-resistance from yeast to primates, making CR an attractive strategy for organ protection in the clinic. Translation of CR to patients is complex, due to problems regarding adherence, feasibility and safety concerns in frail patients. Novel tailored dietary regimens, which modulate the dietary composition of macro- and micronutrients rather than reducing calorie intake promise similar protective effects and increased translatability. However, a direct head-to-head comparison to identify the most potent approach for organ protection as well as overlapping metabolic consequences has not been performed. We systematically analyzed six dietary preconditioning protocols - fasting mimicking diet (FMD), ketogenic diet (KD), dietary restriction of branched chained amino acids (BCAA), two dietary regimens restricting sulfur-containing amino acids (SR80/100) and CR - in a rodent model of renal ischemia-reperfusion injury (IRI) to quantify diet-induced resilience in kidneys. Of the administered diets, FMD, SR80/100 and CR efficiently protect from kidney damage after IRI. Interestingly, these approaches show overlapping changes in oxidative and hydrogen sulfide (H_2S)-dependent cysteine catabolism as a potential common mechanism of organ protection. Importantly, these metabolic changes can be recapitulated in patients preconditioned by a diet limiting sulfur-containing amino acids indicating conserved diet-induced mechanisms of stress-resistance that may ultimately lead to clinical application.

Introduction

Recent research has greatly improved our knowledge on longevity pathways and holds the promise to yield strategies that will allow for healthy aging in humans. Dietary protocols are among the most potent lifespan-extending interventions. Caloric Restriction (CR) - the simplest dietary longevity protocol - has been extensively studied and its effectiveness has been confirmed in a wide range of organisms ranging from budding yeast to rhesus monkeys (1, 2). This is a pivotal pre-requisite for potential translation to human medicine (3, 4). Mechanistically, the activation of longevity pathways leads to an increase in cellular and organismal stress-resistance (1, 5).

Regarding human disease, exploitation of this aspect is an important goal of translational research to protect organ function, when patients are exposed to damaging stimuli (e.g., surgery, ischemia, drug toxicity) in the clinical setting. In this context, the protection from acute kidney injury (AKI) is an important example. Being an aging-associated disease, the incidence of AKI has risen over the last decades (6). AKI is associated with increased mortality and morbidity and promotes progression to chronic kidney disease which, in turn, reduces both life expectancy and quality of life (7). Despite the considerable burden associated with AKI, both effective therapeutic and preventive measures are currently lacking. Interestingly, CR strongly protects from kidney damage in different rodent models of AKI (8-10). However, successful translation of dietary interventions into the clinical setting faces various obstacles partly due to problems regarding adherence, feasibility and safety concerns in frail patients. Consequently, developing tailored dietary interventions that are safe and feasible, but effective in high-risk patients is an important goal. Furthermore, an improved understanding of the molecular and metabolic mechanisms underlying the protective potential of different dietary regimens will be required to allow for the design of pharmacological strategies augmenting resilience.

4

Recent research has provided an insight into targeted dietary regimens, which - instead of reducing calorie intake - modulate the dietary composition of macro- and micronutrients (1, 11, 12). The fasting mimicking diet (FMD) mimics periodic fasting and enables the activation of cellular signal transduction similar to CR, such as a decrease in insulin, leptin and insulin growth factor 1 (IGF-1) (13-15). Furthermore, FMD reduces autoimmunity, inflammation and oxidative stress as well as it promotes autophagy resulting in cellular stress-resistance (11, 16). Ketogenic diets (KD) are high in fat and very low in carbohydrates and result in the synthesis of ketone bodies, such as β-hydroxybutyrate, exceeding β-oxidation of fatty acids as well as suppressing both inflammation and oxidative stress (17, 18). Considering that CR in rodents actually induces ketogenesis due to the resulting feeding cycles and fasting itself, the examination of the protective properties of ketogenic diet are warranted (19). Dietary inhibition of the mechanistic Target of Rapamycin (mTOR) pathway is achieved when the branched chain amino acids (BCAA) valine, leucine and isoleucine are limited (12, 20). mTOR inhibition is known to result in augmented cellular stress-resistance by reducing protein translation and decreasing proteotoxic and oxidative stress (21, 22). In addition, restriction of the sulfur-containing amino acids (SAA) methionine and cysteine is an attractive target to mimic the nephroprotective effect of CR (23). Depletion of methionine and/or cysteine has been widely studied in various longevity model organisms and can be achieved by consuming SAA free or low-SAA foods such as fruit, refined grains and vegetables in humans (12, 24). Reduction of SAA leads to an increase in lifespan and improves metabolic health observed across taxa (1). The balance between methionine and cysteine is regulated by the trans-sulfuration pathway (TSP) and SAA restriction is associated with anti-inflammation, increased stress-resistance, reduction of reactive oxygen species, decline in insulin signaling and alteration in lipid-metabolism (12, 25, 26). All the described dietary approaches have been studied with respect to feasibility and safety in clinical trials or are already in clinical use (14, 27-31). Thus, their

100   administration as a preconditioning strategy in the clinical setting could add substantially to

101   our therapeutic armamentarium. However, systematic analyses on the power and efficacy of

102   different dietary approaches are limited and a direct comparison of these protocols is lacking.

103   While CR has been studied extensively in rodent models of kidney injury, FMD, KD and

104   BCAA restriction have not been examined in this regard (8-10). Addition of SAA to protein-

105   restricted dietary regimens has been shown to abrogate the protective potential, however, SAA

106   restriction itself has not been tested to date (23). Besides, underlying metabolic patterns of

107   protective strategies have not been compared and knowledge on their conservation in humans

108   is limited.

109   Consequently, we set out to perform a simultaneous comparison of six dietary interventions

110   (FMD, KD, BCAA, SR80/100 - two dietary regimens either reducing sulfur-containing amino

111   acids (SAA) by 80 percent (SR80) or fully depleting them (SR100) and CR) in a murine model

112   of AKI. Besides, profiling of metabolites and proteomics were employed to provide an insight

113   into the molecular mechanisms underlying dietary organ protection. Analyses in a human

114   cohort were used to confirm evolutionary conservation of the metabolic response.

Results

Weight development and baseline kidney function in dietary preconditioned and non-preconditioned mice

To examine the diet-induced changes in phenotype and functional kidney parameters, mice were treated with the different dietary regimens (CR, FMD, the low-SAA diets SR80/100, KD and BCAA) for 14 days, sacrificed and compared to *ad libitum* fed, non-preconditioned (non-PC) animals. CR and SR100 mice lost weight significantly, whereas KD mice gained weight compared to non-PC mice. Treatment with FMD, SR80 or BCAA did not result in any weight differences (Fig. S1A). Renal function was assessed by measuring serum creatinine and serum urea and there were no differences in creatinine across all dietary regimens. CR - in line with previously published data - led to a significant increase and KD to a significant decrease in serum urea compared to the non-PC group after 14 days of exposure to the dietary regimens (9). FMD, SR80/100 and BCAA did not reveal significant changes in serum urea (Fig. S1B, C). Additionally, none of the diets had an impact on kidney tissue morphology as determined through a blinded analysis of periodic acid–Schiff (PAS)-stained paraffin-embedded tissue (Fig. S1D, E) (32, 33). Furthermore, we did not observe any diet-related changes of general health, behavior or activity of the mice.

Tailored dietary preconditioning improves survival and general health status in mice after renal IRI

To induce AKI, we performed right nephrectomy and exposed the left kidney to IRI in male C57BL/6N mice after dietary preconditioning and respective controls. CR and the non-PC group served as positive and negative controls, respectively. Sham animals, which underwent right nephrectomy without clamping of the vascular pedicle of the contralateral kidney, did not develop AKI and served as an additional control for the surgical setting (Fig. 1A).

140   Preconditioning with FMD, SR80/100 and CR led to significantly improved survival following

141   AKI (*P < 0.0001*). None of these animals died or had to be euthanized according to previously

142   defined criteria within 72 hours after renal IRI, whilst this was the case for 50% of the non-PC

143   animals. Two out of 13 (15.4%) and nine out of 13 (69.2%) animals had to be sacrificed or

144   died within 72 hours after renal IRI in the KD and the BCAA group, respectively (Fig. 1B).

145   Moreover, animals in the SR100 and the CR group gained weight within 72h, whereas FMD,

146   SR80, KD, BCAA, non-PC and even sham animals lost weight after surgery (Fig. 1C). In line

147   with the survival benefit, mice preconditioned with FMD, SR80/100, KD or CR showed an

148   improved overall health status both 24(Table S1, Fig. S2).

149

150   **FMD and SR80/100 recapitulate CR benefits in maintaining kidney function following**

151   **IRI**

152   Kidney damage of the different groups was quantified by measuring serum creatinine and

153   serum urea at 24 hours and 72 hours after renal IRI. At 24 hours, FMD, SR100 and CR showed

154   significantly lower creatinine values compared to the non-PC group, whilst creatinine did not

155   differ between non-PC, SR80, KD and BCAA (Fig. 1D). Regarding serum urea,

156   preconditioning with SR100 and CR significantly attenuated the increase observed at 24 hours

157   after IRI, whereas FMD, SR80, KD and BCAA did not lead to a significant difference in serum

158   urea compared to the non-PC group (Fig. 1E). With regard to the later time-point 72h after IRI,

159   in contrast to non-PC animals, kidney function returned to near normal in FMD, SR80/100 and

160   CR mice. Regarding mice on KD, only serum urea levels were significantly lower than in non-

161   PC animals. With respect to serum creatinine levels, KD preconditioned mice apparently split

162   into two groups. BCAA preconditioning did not result in any signs of renal protection (Fig. 1F,

163   1G). The sham intervention did not have any impact on kidney function (Fig. 1 D-G).

164   When compared to baseline values obtained from mice that were sacrificed after the

165   preconditioning phase (i.e., before surgery), creatinine concentrations were not significantly

166   elevated at 24 hours and 72 hours after IRI in CR or SR100 preconditioned mice (Fig. S3A).

167   SR100 preconditioned mice showed slightly elevated serum urea values at 24 hours, whilst

168   there was no significant rise at 72 hours (Fig. S3B). CR mice did not differ significantly in

169   serum urea at 24 hours, however, CR resulted in elevated values already at baseline (Fig. S1C).

170   FMD and SR80 preconditioned mice revealed mildly impaired kidney function at 24 hours

171   after renal IRI as indicated by an increase in both serum creatinine and urea at this time-point

172   compared to respective baseline animals. However, at 72 hours after IRI, kidney function was

173   almost completely restored in FMD and SR80 animals (in SR80 serum urea remained slightly

174   elevated). In contrast, KD- and BCAA-preconditioned, as well as non-PC mice revealed a

175   severely impaired kidney function at all examined points in time compared to respective

176   baselines animals (Fig. S3).

177

178   **FMD, SR80/100 and CR strongly attenuate cellular damage after renal IRI**

179   To assess damage in epithelial cells of the renal tubular system after IRI, we used an established

180   semi-quantitative histologic damage score integrating epithelial flattening, loss of brush

181   borders, loss of nuclei, necrosis and vacuolization determined in a blinded manner (32, 33).

182   Direct comparison of the overall damage score identified significantly less acute tubular

183   damage in FMD, SR100 and CR preconditioned mice compared to non-PC animals 24 hours

184   after IRI (Fig. S4A). This protection from kidney damage was mainly driven by the extent of

185   tubular necrosis. Differences in other common signs of tubular damage did not reach statistical

186   significance at this early time-point (Fig. S4B-G). Neither the overall score nor necrosis

187   quantified in KD and BCAA animals differed from non-PC mice 24S4A, S4F, S4GFMD, the

188   low-SAA diets SR80/100 and CR mice sacrificed at 72 hours after IRI were significantly

189   protected from renal damage quantified by histology (Fig. 2A). Again, this result was primarily

190   caused by differences in the extent of tubular necrosis (Fig. 2B, S5A-S5D). However, SR100

191   animals additionally revealed significantly less loss of brush borders compared to non-PC mice

192   at this time-point (Fig. S5C). To perform a longitudinal analysis after renal IRI within each

193   group, damaged kidneys obtained at 24 hours and 72 hours after IRI were also compared to

194   baseline animals of the respective dietary group confirming the protective effects. In contrast,

195   in KD, BCAA and non-PC mice acute tubular damage significantly worsened over time after

196   renal IRI, both when compared to non-PC kidneys or the respective baseline tissue (Fig. 2, S4,

197   S5). To further analyze the degree of cell death, we performed immunostaining of cleaved-

198   caspase-3 and deoxynucleotidyl transferase–mediated dUTP nick end-labeling

199   assay (TUNEL) (34, 35). Immunostaining of cleaved-caspase-3 suggested severe cellular

200   damage in non-PC and BCAA mice, whereas KD showed a less profound staining. FMD, the

201   low-SAA diets SR80/100 and CR animals showed (almost) no anti-cleaved-caspase-3 positive

202   staining pattern (Fig. S6). TUNEL staining demonstrated high numbers of positive cells in

203   BCAA and non-PC animals, significantly less in KD and SR80 animals and hardly any signal

204   in FMD, SR100 and CR animals (Fig. 2D).

205

206   **FMD, SR80/100 and CR modulate oxidative cysteine and hydrogen sulfide metabolism**

207   **with a central role for sulfite**

208   CR promotes the H_2S-generating branch of cysteine metabolism (TSP) resulting in the

209   generation of H_2S, which has been shown to be a mediator of CR-induced stress resistance (23).

210   Supplementation of sulfur-containing amino acids counteracts the CR-orchestrated benefits in

211   rodents (23). Based on this knowledge, we inspected the four most potent dietary regimens

212   (FMD, SR80/100 and CR) regarding their impact on cysteine metabolism in post-diet pre-IRI

213   mice. Targeted quantification by high performance liquid chromatography (HPLC) revealed a

10

214   significant elevation of serum cysteine after FMD and, surprisingly, also in the cysteine-free

215   diet SR100. The increase observed in the SR80 group did not reach statistical significance and

216   CR did not change serum cysteine compared to the *ad libitum* fed non-PC group (Fig. 3A). In

217   contrast, serum homocysteine was commonly reduced at baseline after FMD, the low-SAA

218   diets and CR compared to non-PC animals indicating cysteine turnover (Fig. 3B).

219   Next, we characterized metabolites of cysteine catabolism in more detail by quantifying

220   s-sulfocysteine (SSC), thiosulfate and sulfite levels. SSC and thiosulfate are two major end-

221   products of the cysteine catabolism, whilst sulfite serves as a common intermediate of both

222   catabolic pathways and precursor of SSC (Fig. 4). Urine sulfite measurements revealed

223   significantly elevated levels in both FMD and CR as compared to non-PC animals. In contrast,

224   we found a decrease in urine sulfite in the low-SAA diets (Fig. 3C). Of note, SR80/100 resulted

225   in a profound rise in urine SSC as compared to non-PC animals with no significant difference

226   between the two SAA restricted regimens, an effect that was neither induced by FMD nor CR

227   (Fig. 3d). SSC is generated by the non-catalyzed reaction of cystine and sulfite and is widely

228   used as a biomarker for sulfite levels indicating elevated sulfite signaling in low-SAA diets.

229   Increased turnover of sulfite towards cysteine and SSC may explain both the reduced urine

230   sulfite levels and the lack of a reduction (SR80) or even rise (SR100) in serum cysteine

231   observed upon dietary SAA restriction (Fig. S7).

232   Thiosulfate - another end-product in H_2S-dependent cysteine metabolism - is generated by H_2S

233   catabolism in a sulfite-dependent manner. We found significantly increased serum thiosulfate

234   levels after FMD and SR80/100 as well as a strong trend towards elevated serum thiosulfate

235   levels in CR animals ($P = 0.08$) compared to non-PC animals (Fig. 3e). Conclusively, FMD,

236   low-SAA diets and CR result in a commonly shared activation of both oxidative and H_2S-

237   dependent cysteine catabolism as demonstrated by elevated thiosulfate, sulfite and SSC (Fig.

238   S7).

239

SR100 results in a reciprocal regulation of H_2S-synthesizing enzymes MPST and CBS

We used quantitative proteome profiling to decipher changes of key enzymes in the TSP in kidney in response to SAA depletion and FMD (Fig. 4, S7, S8, Table S2). Interestingly, SR100 - but none of the other regimens - lead to upregulation of MPST that catalyzes the desulfuration of 3-mercaptopyruvate (3-MP) and transfers sulfane sulfur to its thiophilic acceptors resulting in release of H_2S. This increase in MPST, was accompanied by a significant decrease of CBS levels in response to low SAA levels, whereas there was no significant change in CTH, the known TSP enzymes involved in H_2S biosynthesis.

Independent from the H_2S-generating branch, cysteine is metabolized via two other distinct pathways, the γ-glutamylcysteinylglycine dependent synthesis of glutathione and the branch leading to the formation of either taurine or sulfate. Of interest, the key enzymes in both glutathione, as well as taurine synthesis, GSS and CSAD, respectively, were significantly downregulated in our animals in response to SR100 (Fig. 4, Table S2). Taken together, dietary SAA depletion results in a profound modulation of key enzymes within cysteine metabolism in favor of MPST-dependent activation of the H_2S-generating branch in murine kidneys.

255

FMD leads to an upregulation of CDO1 and higher expression levels of GOT1/2 in oxidative and H_2S-dependent cysteine catabolism

CDO1 is the first and rate-limiting enzyme in oxidative cysteine catabolism and converts cysteine to cysteine sulfic acid (CSA). FMD resulted in a strong upregulation of CDO1 (Table S2). CDO1 is tightly regulated in cysteine homeostasis and elevated levels of CDO1 correlate with increased cysteine abundance accompanied by an activation of oxidative cysteine catabolism. In line with the marked increase in CDO1, the expression levels of the downstream targets GOT1/2 were also elevated in response to FMD; however, this

264 upregulation was less strong and less significant (Fig. S8, Table S2). GOT1 has been shown

265 recently to function in CSA deamination leading to sulfite, while GOT2 is part of an MPST-

266 dependent pathway resulting in the generation of H_2S (Fig. 4) (36).

267

268 **Proteome profiling identifies overlapping regulation of autophagy associated proteins in**

269 **beneficial diets**

270 To decipher overlapping diet-mediated molecular changes beyond cysteine and H_2S

271 metabolism, we performed a global quantitative analysis of the proteome data. Principal

272 component analysis revealed the most profound separation for FMD, SR100 and CR animals

273 from non-PC mice, whereas kidneys after preconditioning with SR80, KD and BCAA tended

274 to be more similar (Fig. S9A). To identify common patterns in dietary regimens that were

275 clearly associated with renal organ protection we compared FMD, SR80/100 and CR in more

276 detail. These protocols induced differential regulation of 176, 87, 377 and 132 proteins

277 compared to non-PC animals (Fig. S9B). A significant overlap was observed in 48 proteins that

278 were differentially expressed in kidneys in response to at least three of these dietary strategies.

279 Seven proteins (ATG7, BCR, CTPS2, KCNJ16, PRKA, SPATA5, TMEM256) revealed a

280 shared mode of regulation after dietary preconditioning with FMD, SR80/100 and CR

281 compared to non-PC animals (Fig. S9C). Of note, three commonly regulated proteins (ATG7,

282 CTPS2, PRKA) are associated with cellular processes in autophagy.

283

284 **Generation of SSC and elevated sulfite metabolism are induced by a low-SAA diet in**

285 **humans**

286 To confirm whether molecular mechanisms obtained by low-SAA diets are conserved in

287 humans, changes in cysteine catabolism were analyzed in a pilot-cohort of ten participants that

288 underwent dietary SAA restriction using a formula diet for seven days compared to ten age-

289 and sex-matched individuals on a formula diet containing standard levels of SAA (Table S3).

290 To decipher changes in cysteine catabolism upon dietary SAA restriction in humans we

291 quantified serum cysteine, serum cystine und urinary SSC levels in the low-SAA and the

292 control group. In line with our findings from the rodent studies, pre- and post-diet cysteine

293 levels, as well as the individual turnover in cysteine did not differ between the two groups even

294 though SAA were heavily restricted (Fig. 5A-C). As cystine reacts with sulfite to generate SSC

295 and cysteine, we detected significant lower levels of serum cystine in response to the low-SAA

296 group, however, the individual fold change did not reach statistical significance (Fig. 5D-

297 F) (37). Urinary SSC levels, a major side-product of sulfite elevation, did not differ between

298 the low-SAA and the control group at baseline prior to dietary intervention (Fig. 5G, 5J). Of

299 interest and consistent with our rodent data, participants in our pilot-cohort receiving the SAA-

300 restricted diet had significantly higher urinary SSC levels in both spontaneous samples and 24h

301 urine collections after short term dietary intervention (Fig. 5H, 5K). Besides, the individual

302 increase of urinary SSC was significantly higher in the low-SAA group (Fig. 5I, 5L).

303 Considering the significant findings regarding SSC and its central role in the H_2S-producing

304 branch of cysteine catabolism, we went on to measure SSC in a larger group of patients (n=49)

305 after SAA restriction. Again, pre-dietary levels of urinary SSC did not differ (Fig. 6A) and we

306 observed a significant rise in urinary SSC in response to the low-SAA diet indicating active

307 cysteine catabolism (Fig. 6B, 6C).

308 Conclusively, we could recapitulate adaptions in cysteine and sulfite metabolism in humans

309 upon a low-SAA diet indicating conserved diet-induced mechanisms of stress-resistance.

310

Discussion

Impaired cellular stress-resistance contributes to various diseases including common and life-threatening AKI, a frequent age-associated complication. Although CR effectively augments resilience leading to amelioration of AKI and superior survival rate in rodent models, a better understanding of the underlying mechanisms is required for successful clinical translation (8-11, 28, 38). Based on recent results regarding novel dietary regimens derived from longevity studies in animal models, five tailored dietary interventions were considered promising for the prevention of AKI beyond CR and their efficacy was systematically examined in a direct comparison (13, 14, 18, 20, 25, 39, 40). All five interventions had not been studied as protective strategies against AKI before and had never been directly compared to identify the most potent approach as well as associated metabolic patterns.

Regarding kidney function, survival, general health status and tissue damage, we identified FMD, and the low-SAA diets SR80/100 as the most potent preconditioning strategies beyond CR (32, 33). KD revealed less profound protective effects, but was indeed accompanied by improvements in survival and general health. In contrast, dietary mTOR inhibition by BCAA restriction failed to protect from renal ischemic damage and did not improve any of the indicators examined. Despite its beneficial effects on lifespan, inhibition of mTOR activity during the reperfusion in renal IRI using rapamycin has been shown to slow down kidney recovery after AKI, which may also explain the failure in renal protection by BCAA preconditioning we observed (41).

Considering that a reduction of SAA was among the most efficient approaches, we decided to examine the impact of the protective regimens on the TSP and cysteine metabolism. TSP enzyme-mediated generation of H_2S is evolutionary conserved and plays a pivotal role in augmenting cellular stress-resistance and healthspan extension (1). The well-known protective effects of CR in ischemic hepatic damage, for example, are - at least in part - conveyed by the

15

336   modulation of cysteine catabolism and production of H_2S (23). The primary source of H_2S

337   generation are various metabolites that arise from cysteine metabolism. In addition to the H_2S-

338   producing branch, there are two further pathways involved in cysteine metabolism,

339   (i) oxidative cysteine catabolism to taurine or sulfate and (ii) glutathione biosynthesis.

340   Mechanistically, supplementation of the SAA methionine and cysteine abrogates the increased

341   production of H_2S and counteracts CR-mediated stress-resistance in rodents (23).

342   The most potent dietary regimens in our study - FMD, SR80/100 and CR - resulted in strong

343   adaptations in oxidative and H_2S-dependent cysteine catabolism. Despite the fact that the

344   changes upon all of these four regimens point towards an overall increase in cysteine

345   catabolism, the underlying mechanisms may differ as indicated by the distinct alterations of

346   cysteine, homocysteine, sulfite, SSC and thiosulfate. All beneficial diets induce an elevation in

347   serum thiosulfate with FMD showing the highest and most significant rise (>3fold).

348   Importantly, elevated thiosulfate is a direct proxy for increased H_2S turnover (23). This rise in

349   thiosulfate after FMD is accompanied by a reduction in homocysteine and an elevation in

350   cysteine, revealing a flux towards cysteine. Moreover, elevated levels of sulfite and thiosulfate

351   indicate increased oxidative and H_2S-dependent cysteine catabolism in response to its

352   abundance after FMD. We could recapitulate the FMD-induced activation of oxidative cysteine

353   catabolism on the protein level and show a strong upregulation of the initial and rate-limiting

354   enzyme CDO1 - a prerequisite for the production of sulfite (Fig. 4). Furthermore, we identified

355   an increase of the downstream enzymes GOT1/2 in response to FMD that directly accept

356   cysteine and cysteine sulfinate for transamination contributing to H_2S and sulfite generation,

357   respectively, and are, consequently, both required for thiosulfate formation (Fig. 4, S8) (36).

358   Similarly, both low-SAA diets revealed a rise in serum thiosulfate indicating the generation of

359   H_2S accompanied by an upregulation of MPST after SR100. As MPST desulfurizes 3-MP and

360   transfers sulfane sulfur to its thiophilic acceptors, H_2S is released. This rise in MPST was

16

361 accompanied by a downregulation of key enzymes in cysteine catabolism outside the H_2S-

362 dependent branch, CSAD and GSS, leading to a shift in favor of the H_2S-generating

363 pathway (Fig. 4). However, in contrast to FMD and CR, SR100 resulted in a significant

364 decrease of sulfite. While this may appear counterintuitive at first sight, our further metabolite

365 quantifications provide a reasonable explanation for this finding. Of note, both low-SAA diets

366 resulted in a substantial increase of urinary SSC, a secondary end product induced upon sulfite

367 elevation. SSC is generated through the spontaneous, non-catalyzed reaction of sulfite with

368 cystine and is widely used as a biomarker for sulfite levels (37, 42). High SSC values measured

369 in SR80/100 indicate that the sulfite-producing H_2S catabolism is indeed not only activated by

370 FMD and CR but also by low-SAA diets. During the formation of SSC from sulfite and cystine,

371 cysteine is released explaining the missing reduction (SR80) or even the rise in cysteine

372 (SR100), even though dietary SAA supply was heavily reduced (Fig. S7) (43). Furthermore,

373 this reaction also provides an explanation for the low sulfite levels observed in SR80/SR100

374 treated animals. This reciprocal relation of low sulfite and elevated SSC is not seen in CR and

375 FMD diets.

376 Importantly, we confirmed diet-induced metabolic adaptations in cysteine metabolism in

377 human bio-samples after SAA restriction. The rise in SSC generation was accompanied by a

378 reduction in serum cystine and maintained cysteine levels upon dietary restriction of SAA in

379 our pilot-cohort. This reduction in cystine is likely to be a consequence of its reaction with

380 sulfite indicating active sulfite metabolism and cysteine maintenance as a shared pattern

381 between rodents and humans in response to low-SAA diets. Sulfite is a common intermediate

382 in oxidative and H_2S-dependent cysteine catabolism and contributes to the reported H_2S related

383 signaling effects in cellular stress-resistance, i.e. by liberating H_2S when reacting with

384 persulfides (44-46). Additionally, sulfite itself is known to mediate cytoprotective effects by

385 e.g., scavenging of reactive oxygen (ROS) and nitrogen species (RNS) or maintaining levels

386 of cysteine and glutathione (1, 44, 45).

387 Currently, it remains unclear whether the benefits of an elevated cysteine catabolism including

388 sulfite and H_2S generation require a simultaneous increase in autophagy (23). In yeast,

389 longevity benefits by methionine restriction are based on autophagy, whereas in mammals this

390 remains unknown (47). Interestingly, we found strong hints using comparative proteome

391 profiling, that FMD, SR80/100 and CR interfere with autophagy-associated genes in a similar

392 fashion. Of note, three of the seven overlapping proteins (ATG7, PRKA and CTPS) that are

393 differentially regulated by all of these four diets contribute to autophagy. Interestingly,

394 conditional ATG7 ablation from proximal tubules aggravates AKI, whereas activation of

395 autophagy protects from AKI (48, 49). The PKR (also named EIF2AK2) axis is activated by

396 PRKA in the absence of double-stranded RNA (dsRNA), which is found during endoplasmic

397 reticulum stress and in settings of insulin resistance (50). Conversely, low PRKA levels and a

398 downregulated PKR pathway induce autophagy and protect from inflammation and oxidative

399 stress (51). CTPS2, one of the two isoforms of the CTP synthase, is the key regulatory enzyme

400 in pyrimidine biosynthesis. Interestingly, CTPS2 has an essential role in the maintenance of

401 genome integrity and the synthesis of membranes (52).

402 Our study has several limitations: First, findings from our rodent IRI-model may not entirely

403 reflect the pathogenesis of AKI in the clinical setting. Second, due to restraints regarding their

404 production, SR80/100 and BCAA have an altered macronutrient ratio compared to the standard

405 chow, which may additionally influence the given results. Third, as male rodents are more

406 vulnerable to IRI we only examined male animals. Consequently, sexual dimorphism regarding

407 dietary interventions is not reflected by our study. However, this aspect may also differ between

408 mice and humans since the sex-related differences in susceptibility generally observed in mice

409 are not obvious in available human data (39, 53). Fourth, direct pharmacological manipulation

410   of sulfite and H_2S would be an attractive target for clinical translation and will need to be

411   addressed in follow-up studies (54).

412   Regarding our human data, the limited number of participants in our pilot-cohort recapitulating

413   the observed metabolic adaptions of the beneficial diets has to be acknowledged. Furthermore,

414   the dietary intervention was executed in an outpatient setting associated with potential issues

415   regarding adherence. Nonetheless, the key finding regarding SSC was indeed confirmed in a

416   larger cohort.

417   In conclusion, our systematic and direct comparison of five tailored dietary preconditioning

418   regimens identified FMD and SAA-restriction as highly potent strategies for organ protection

419   beyond CR. We identified modulation of cysteine catabolism as a pivotal common aspect of

420   these interventions with sulfite metabolism as its central component. The impact of SAA-

421   restriction on cysteine metabolism could be confirmed in a human cohort. Since both FMD and

422   low-SAA diets are feasible in humans our findings provide an important outlook towards novel

423   protective strategies in the patient setting. Besides dietary interventions, pharmacological

424   modulation of oxidative and H_2S-dependent cysteine catabolism may be exploited in the future.

425

426 **Methods**

427 **Dietary Preconditioning in Rodents**

428 Male C57BL6N mice were obtained at 6 weeks of age from Janvier Labs (Paris, France) and

429 maintained individually upon arrival in an identical specific pathogen free environment with

430 constant temperature and humidity and 12h/12h light/dark cycle. Unless otherwise on specific

431 experimental diets, mice were fed *ad libitum* with their regular chow (V155-330 ssniff GmbH,

432 Soest, Germany) and had unrestricted access to water.

433 Male C57BL6N mice aged 8 weeks were allocated randomly to their specific dietary regimen

434 and transferred to a fresh cage at beginning of dietary preconditioning. FMD, SR80/100, KD,

435 BCAA and CR were performed for 14 days prior to renal IRI simultaneously (Fig. 1A). Rodent

436 periodic fasting with FMD is a 3-day regimen and was performed as previously described (13,

437 14). Day 1 of FMD (S5159-E736, ssniff GmbH, Soest, Germany) consists of a combination of

438 flavored broth mixes, vegetable powders, extra virgin olive oil (EVOO), essential fatty acids,

439 minerals and vitamins, whereas on day 2-3 of FMD a combination of flavored broth mixes,

440 glycerol and hydrogel were supplied to the mice (S5159-E738, ssniff GmbH, Soest,

441 Germany) (Table S4). On day 4-7 of FMD mice had *ad libitum* access to their standard chow.

442 Energy intake was reduced to 7.67 kJ/g on day 1 and 1.48 kJ/g on day 2-3 of FMD,

443 respectively. Rodent FMD regimen was performed twice before renal IRI and rodent surgery

444 was performed after the second period with an *ad libitum* access to the standard chow on day

445 14. KD (S51519-E730, ssniff GmbH, Soest, Germany) contained 10% protein, 89% fat and

446 0.6% carbohydrates and mice were supplied with KD daily and had *ad libitu*m access to the

447 high-fat chow (Table S5). BCAA chow (S5159-E724, ssniff GmbH, Soest, Germany) resulted

448 in a 66% reduction of leucine, isoleucine and valine as previously described (20). To reduce

449 the daily uptake of SAA, either a full restriction of methionine and cysteine (SR100, S5159-

450 E720, ssniff GmbH, Soest, Germany) or an 80%-reduction of SAA (SR80, S5159-E722, ssniff

451   GmbH, Soest, Germany) were used (Table S5). BCAA and the low-SAA diets SR80/100 were

452   supplied weekly and mice had *ad libitum* access to the respective chow. Animals

453   preconditioned by CR received 70% of the regular daily intake (3g/d) of their regular chow for

454   14 days prior to renal IRI and they were supplied with food in the morning hours (9.00 - 11.00

455   am) on each day during dietary regimen. Food intake for CR animals was chosen based on

456   previous rodent studies examining CR in the context of AKI (9, 10). CR animals were not fed

457   on the day of surgery.

458   During dietary preconditioning mice had *ad libitum* access to water and they consumed all

459   supplied diets revealing no signs of food aversion. To assess weight loss mice were weighted

460   weekly and no increase in morbidity or mortality was observed during any of the dietary

461   interventions.

462

463   **Renal Ischemia-Reperfusion Injury Model**

464   To induce AKI, a warm renal ischemia-reperfusion ischemia (IRI) model as previously

465   described with slight modifications was used (9). Briefly, to perform surgery, mice were

466   anesthetized with i.p. administered ketamine (Zoetis Inc. Parsipanny, NJ, USA) / xylazine

467   (Bayer AG, Leverkusen, Germany). A thermometer was inserted rectally and mice were placed

468   on a temperature-controlled heating pad (Havard apparatus, Holliston, MA, USA) to maintain

469   body temperature. After midline laparotomy the right kidney was removed and the left renal

470   vessels were clamped for 40 minutes with an atraumatic micro-vascular clamp. Renal ischemia

471   was verified visually by color change of the kidney and afterwards the abdomen was covered

472   with a compress soaked in 0.9% saline solution. After restoration of renal blood flow was

473   inspected visually, the abdomen was closed in two layers and the mice were placed in a fresh

474   cage. For analgesia the mice received buprenorphine (Indivior Europe Limited, Dublin,

475   Ireland), in a dosage of 0.1mg/kg per body weight injected s.c. twice daily, as well as

476   0.009mg/mL buprenorphine administered in their drinking water. After surgery, dietary

477   preconditioned and non-PC mice had *ad libitum* access to the standard chow.

478   CR served as positive control, non-PC animals as negative. Another experimental control

479   consisted of sham animals, which underwent right nephrectomy without clamping of the

480   vascular pedicle of the contralateral kidney.

481   Mice were euthanized after 24 hours or 72 hours after reperfusion. Therefore, mice were

482   anesthetized with i.p. ketamine / xylazine injection and final blood withdrawal was performed

483   by puncture of the right ventricle. Intraoperative and postoperative obtained kidneys were cut

484   into two equal sections, which were either snap frozen in liquid nitrogen or fixed in

485   4% formaldehyde and subsequently embedded in paraffin, respectively. Baseline animals were

486   sacrificed by final blood drawing after dietary interventions but before renal IRI. Both kidneys

487   were cut into two equal sections and these were either snap frozen in liquid nitrogen or fixed

488   in 4% formaldehyde with subsequent paraffin embedding. Mouse urine was directly snap-

489   frozen in liquid nitrogen upon collection. Mouse urine and serum samples were stored at -80°C.

490

491   **Renal Function and Health Performance after Renal Ischemia-Reperfusion Injury**

492   Mouse serum creatinine and urea levels were measured by the central laboratory of the

493   University Hospital Cologne using a Cobas C 702 (Roche Diagnostics GmbH, Penzberg and

494   Mannheim, Germany). Postoperative health performance was examined in the morning hours

495   (9.00 - 11.00 am) of each day using a governmental authorities approved recovery score that

496   consisted of weight loss, appearance and activity (Table S1). Mortality and postoperative

497   recovery were assessed over a period of 72 hours after renal IRI.

498

499   **Histopathology**

500 Formalin-fixed, paraffin-embedded tissue was cut into 2-µm-thick slices and stained with

501 periodic acid–Schiff (PAS). Acute tubular damage was classified in a semi-quantitative and

502 blinded manner by an experienced nephropathologist (H.G.) using a composite score assessing

503 vacuolization, epithelial flattening, loss of either brush borders or nuclei and tubular

504 necrosis (32, 33). According to the affected area grades were given from 0-4 (1: 0%–25%, 2:

505 25%–50%, 3: 50%–75%, 4: 75%–100%). Images of PAS-staining were obtained using a slide

506 scanner SCN4000 (Leica, Wetzlar, Germany) in a 20× magnification.

507

508 **Terminal Deoxynucleotidyl Transferase–Mediated Digoxigenin-Deoxyuridine Nick-End**

509 **Labeling Staining**

510 DeadEnd Fluorometric TUNEL System (Promega, Fitchburg, WI, USA) was used on 2 µm

511 thick formalin-fixed paraffin sections according to the manufacturer's protocol. Images were

512 taken on an Axiovert 200M microscope with a Plan-Apochromat 20×/0.8 objective and an

513 AxioCamMR camera (all Carl Zeiss MircoImaging GmbH, Jena, Germany).

514

515 **Immunohistochemistry**

516 Cleaved-caspase-3 immunostaining was performed on 2 µm thick formalin-fixed paraffin

517 sections in a 1:200 dilution according to the manufacture's protocol (Cell Signaling

518 Technology, Danvers, MA, USA). Pictures were taken on a slide scanner SCN4000 in a 20×

519 magnification.

520

521 **Human samples**

522 Human biosamples were collected from patients participating in a randomized placebo-

523 controlled trial after 7 days of dietary preconditioning using formula diets; trial design is

524 described in detail on clinicaltrials.gov (NCT03715868). Briefly, the control arm was fed a

525   standard liquid formula diet, whilst the intervention arm received a liquid formula diet

526   containing SAA levels reduced by 77%. Participants were randomly assigned to the two

527   treatment groups. Daily caloric intake was not restricted and equal in both groups.

528   Urine creatinine concentrations were measured in the central laboratory of the University

529   Hospital Cologne using a Cobas C 702. All urine-samples for further biochemical analysis

530   were stored at -80°C. Plasma cystine was determined in the central laboratory of the University

531   Hospital Cologne in pre-dietary, as well as post-dietary samples obtained on the seventh day

532   of dietary intervention. Metabolic characterization of cysteine catabolism was performed in a

533   pilot-cohort of ten sex-and age-matched participants. Urinary SSC was additionally quantified

534   as a read-out for cysteine catabolism in a larger cohort of 49 patients adhering to either a low-

535   SAA or control diet.

536

537   **Targeted High-Performance Liquid Chromatography**

538   Cysteine, homocysteine, sulfite, thiosulfate and s-sulfocysteine (SSC) were determined by

539   targeted high-performance liquid chromatography (HPLC). For the detection of cysteine,

540   homocysteine, sulfite and thiosulfate in murine and human serum or urine we chose a

541   monobromobimane (mBBr) derivatization approach. Briefly, defrosted samples were

542   centrifuged and the supernatant were mixed with 4-(2-hydroxyethyl)-1-

543   piperazineethanesulfonic acid (HEPES), ethylenediaminetetraacetic acid (EDTA) and mBBr

544   in acetonitrile. The reaction was performed in the dark and was stopped with methanesulfonic

545   acid (MsOH). Before injection, the samples were diluted with four volumes of the respective

546   0.5% acetic acid used as running buffer A, and transferred into a glass HPLC vail. The samples

547   were then transferred on a 125 x 4.0 mm phase 60RP-Select B LiChroCART 250-4 (Sigma-

548   Aldrich St. Louis, MO, USA) and acetic acid was used as running buffer A, methanol as

549   running buffer B. The gradient was: 0–4 min, 5% B; 4–8 min, 20% B; 8–15 min, 25% B; 15–

550   27 min, 60% B; 27–28 min, 100% B; 28–32 min, 100% B; 32–33 min, 5% B; 33–60 min, 5%

551   B. Dabsylated products were determined spectrophotometrically.

552   SSC was detected using a derivatization reaction with 9-fluorenylmethyloxycarbonyl chloride

553   (Fmoc-Cl) as previously described (55). In brief, murine and human urine were centrifuged

554   and the supernatant was mixed with sodium carbonate / bicarbonate (Na2CO3 / NaHCO3) and

555   Fmoc-Cl in acetonitrile. The derivatization mixture was incubated in the dark and the reaction

556   was stopped through the addition of amantadine-hydrogen chloride (HCl). All samples were

557   centrifuged and the supernatant was transferred into a glass HPLC vial. SSC-Fmoc was

558   separated on a Nucleodur HTec C18 RP column (Macherey-Nagel GmbH, Düren, Germany).

559   Running buffer A was Na-formate, trifluoroacetic acid and running buffer B was methanol.

560   SSC was eluted at 1 mL/min in buffer B at 35-65% and 0-15.0 min gradient, eluting at

561   9.97 min. SSC was quantified based on area under the peak at 265 nm.

562

563   **Absorption-based creatinine determination in mouse urine**

564   Thawed murine urine samples were diluted 1:10 in HCl and transferred together with standard

565   curve of creatinine into individual wells of a 96-well plate. After incubating with alkaline

566   picrate solution in the dark, urine creatinine concentration were determined

567   spectrophotometrically.

568

569   **Proteomic analysis with Liquid Chromatography and Tandem Mass Spectrometry**

570   All samples were analyzed on a Q Exactive Plus Orbitrap mass spectrometer coupled to an

571   EASY nLC 1000 (both Thermo Fisher Scientific, Waltham, MA, USA). Peptides were loaded

572   with solvent A (0.1% formic acid in water) onto an in-house packed analytical column filled

573   with Poroshell EC120 C18 material (Agilent Technologies, Santa Clara, CA, USA). Peptides

574   were chromatographically separated at a constant flow rate of 250 nL/min using the following

575   gradient: 3-4% solvent B (0.1% formic acid in 80 % acetonitrile) within 1.0 min, 4-27% solvent

576   B within 119.0 min, 27-50% solvent B within 19.0 min, 50-95% solvent B within 1.0 min,

577   followed by washing and column equilibration. The mass spectrometer was operated in data-

578   dependent acquisition mode. The MS1 survey scan was acquired from 300-1750 m/z at a

579   resolution of 70,000. The top 10 most abundant peptides were isolated within a 1.8 Th window

580   and subjected to HCD fragmentation at a normalized collision energy of 27%. The AGC target

581   was set to 5e5 charges, allowing a maximum injection time of 55 ms. Product ions were

582   detected in the Orbitrap at a resolution of 17,500. Precursors were dynamically excluded for

583   30.0 s. Raw data were processed with MaxQuant (version 1.5.3.8) using default parameters

584   searching against the canonical *Mus musculus* reference proteome (UP000000589)

585   downloaded on the 26th of August, 2020. Results were further analyzed in Perseus 1.6.1.1 and

586   RStudio (RStudio Inc., Boston, MA, USA) as previously described (10). Briefly, proteins

587   identified by only one site and reverse hits were removed. Label-free quantification of proteins

588   were $\log_2$ transformed and filtered for at least 4 valid measured values being present per dietary

589   group. Two-tailed *t*-tests and two-tailed analysis of variances (ANOVA) were calculated where

590   appropriate. To determine significant proteins and to correct for multiple testing were a FDR

591   was set to 0.05. Functional data were plotted using RStudio and the ggplot2 as well as cowplot

592   packages.

593

594   **Statistics**

595   Statistical analysis was done with GraphPad Prism software version 5 (GraphPad Prism

596   Software Inc. San Diego, CA, USA). Animals were randomly allocated to their dietary

597   preconditioning group. Rodent experiments were not blinded due to the different diets. The

598   histological damage score, biochemistry analyses as well as serum creatinine and serum urea

599   measurements were conducted blinded. Samples sizes were chosen based on experience with

600   previous studies employing renal IRI in rodents (n=10 and n=13 mice per time-point and

601   dietary regimen, respectively) and no power analysis was done to determine samples sizes (8,

602   9). For metabolic and proteome profiling at least four biologic replicates were tested. Ten adults

603   that underwent dietary SAA restriction using a formula diet for seven days compared to ten

604   age- and sex-matched individuals on a formula diet containing standard levels of SAA were

605   used as a pilot-cohort to confirm metabolic adaptions in humans. Human participants were

606   randomly assigned to the two treatment groups in a double-blinded clinical trial. In four adults,

607   spot- and 24h-urine collection of either pre- or post-diet was missing. Urinary SSC was

608   additionally quantified in a larger cohort of 49 patients. No data nor outliers were excluded

609   from the study. Results are depicted as mean ± standard deviation. One-way ANOVA and

610   Bonferroni multiple comparison test were used to examine differences between groups unless

611   otherwise indicated. *P < 0.05* was considered significant.

612

613   **Study approval**

614   All animal procedures were approved by the State Agency for Nature, Environment and

615   Consumer Protection North Rhine-Westphalia, Germany, (TVA2019.A345). The human study

616   protocol was approved by the Institutional Review Board of the University Hospital Cologne

617   and informed consent was obtained from all participants prior to inclusion. Trial design is

618   described in detail on clinicaltrials.gov (NCT03715868).

Author contributions:

F.C.K. and C.Y.F. performed experiments, F.C.K., C.Y.F., M.R.S., K.J.R.H.-A., K.B., H.G., J.S., A.A., G.S., V.B. and R.-U.M. analyzed experiments, F.G., T.O., C.G., R.-U.M. and V.B. contributed human bio-samples, F.C.K., V.B. and R.U.M. designed the study, J.-W.L. and G.S. contributed new tools, F.C.K., G.S, V.B. and R.-U.M interpreted results, F.C.K, G.S., V.B. and R.-U.M. wrote the article. M.R.S., K.J.R.H.-A., F.G., J.S., A.A., T.B., and B.S. revised the manuscript.

644   ground-breaking research in dietary restriction and hydrogen sulfide metabolism, who

645   tragically passed away last year.

646

References and Notes

1. Fontana L, and Partridge L. Promoting health and longevity through diet: from model organisms to humans. *Cell.* 2015;161(1):106-18.

2. Mattison JA, et al. Impact of caloric restriction on health and survival in rhesus monkeys from the NIA study. *Nature.* 2012;489(7415):318-21.

3. Fontana L, et al. Long-term calorie restriction is highly effective in reducing the risk for atherosclerosis in humans. *Proc Natl Acad Sci U S A.* 2004;101(17):6659-63.

4. Heilbronn LK, et al. Effect of 6-month calorie restriction on biomarkers of longevity, metabolic adaptation, and oxidative stress in overweight individuals: a randomized controlled trial. *Jama.* 2006;295(13):1539-48.

5. Fontana L, and Klein S. Aging, adiposity, and calorie restriction. *Jama.* 2007;297(9):986-94.

6. Susantitaphong P, et al. World incidence of AKI: a meta-analysis. *Clin J Am Soc Nephrol.* 2013;8(9):1482-93.

7. Rewa O, and Bagshaw SM. Acute kidney injury-epidemiology, outcomes and economics. *Nat Rev Nephrol.* 2014;10(4):193-207.

8. Mitchell JR, et al. Short-term dietary restriction and fasting precondition against ischemia reperfusion injury in mice. *Aging Cell.* 2010;9(1):40-53.

9. Johnsen M, et al. The Integrated RNA Landscape of Renal Preconditioning against Ischemia-Reperfusion Injury. *J Am Soc Nephrol.* 2020;31(4):716-30.

10. Spath MR, et al. The proteome microenvironment determines the protective effect of preconditioning in cisplatin-induced acute kidney injury. *Kidney Int.* 2019;95(2):333-49.

11. Longo VD, and Mattson MP. Fasting: molecular mechanisms and clinical applications. *Cell Metab.* 2014;19(2):181-92.

12. Brown-Borg HM, and Buffenstein R. Cutting back on the essentials: Can manipulating intake of specific amino acids modulate health and lifespan? *Ageing Res Rev.* 2017;39:87-95.

13. Brandhorst S, et al. A Periodic Diet that Mimics Fasting Promotes Multi-System Regeneration, Enhanced Cognitive Performance, and Healthspan. *Cell Metab.* 2015;22(1):86-99.

14. Choi IY, et al. A Diet Mimicking Fasting Promotes Regeneration and Reduces Autoimmunity and Multiple Sclerosis Symptoms. *Cell Rep.* 2016;15(10):2136-46.

680   15.   Caffa I, et al. Fasting-mimicking diet and hormone therapy induce breast cancer
681   regression. *Nature.* 2020;583(7817):620-4.

682   16.   Madeo F, et al. Caloric Restriction Mimetics against Age-Associated Disease: Targets,
683   Mechanisms, and Therapeutic Potential. *Cell Metab.* 2019;29(3):592-610.

684   17.   Shimazu T, et al. Suppression of oxidative stress by beta-hydroxybutyrate, an
685   endogenous histone deacetylase inhibitor. *Science.* 2013;339(6116):211-4.

686   18.   Roberts MN, et al. A Ketogenic Diet Extends Longevity and Healthspan in Adult Mice.
687   *Cell Metab.* 2017;26(3):539-46.e5.

688   19.   Torres JA, et al. Ketosis Ameliorates Renal Cyst Growth in Polycystic Kidney Disease.
689   *Cell Metab.* 2019;30(6):1007-23.e5.

690   20.   Fontana L, et al. Decreased Consumption of Branched-Chain Amino Acids Improves
691   Metabolic Health. *Cell Rep.* 2016;16(2):520-30.

692   21.   Kapahi P, et al. With TOR, less is more: a key role for the conserved nutrient-sensing
693   TOR pathway in aging. *Cell Metab.* 2010;11(6):453-65.

694   22.   Saxton RA, and Sabatini DM. mTOR Signaling in Growth, Metabolism, and Disease.
695   *Cell.* 2017;168(6):960-76.

696   23.   Hine C, et al. Endogenous hydrogen sulfide production is essential for dietary
697   restriction benefits. *Cell.* 2015;160(1-2):132-44.

698   24.   Gao X, et al. Dietary methionine influences therapy in mouse cancer models and alters
699   human metabolism. *Nature.* 2019;572(7769):397-401.

700   25.   Miller RA, et al. Methionine-deficient diet extends mouse lifespan, slows immune and
701   lens aging, alters glucose, T4, IGF-I and insulin levels, and increases hepatocyte MIF
702   levels and stress resistance. *Aging Cell.* 2005;4(3):119-25.

703   26.   Brown-Borg HM, et al. Growth hormone signaling is necessary for lifespan extension
704   by dietary methionine. *Aging Cell.* 2014;13(6):1019-27.

705   27.   Van Dyck L, et al. Towards a fasting-mimicking diet for critically ill patients: the pilot
706   randomized crossover ICU-FM-1 study. *Crit Care.* 2020;24(1):249.

707   28.   Grundmann F, et al. Preoperative Short-Term Calorie Restriction for Prevention of
708   Acute Kidney Injury After Cardiac Surgery: A Randomized, Controlled, Open-Label,
709   Pilot Trial. *J Am Heart Assoc.* 2018;7(6).

710   29.   Neal EG, et al. The ketogenic diet for the treatment of childhood epilepsy: a randomised
711   controlled trial. *Lancet Neurol.* 2008;7(6):500-6.

712   30.   Hattersley JG, et al. Modulation of amino acid metabolic signatures by supplemented
713   isoenergetic diets differing in protein and cereal fiber content. *J Clin Endocrinol Metab.*
714   2014;99(12):E2599-609.

715   31.   Dong Z, et al. Disease prevention and delayed aging by dietary sulfur amino acid
716   restriction: translational implications. *Ann N Y Acad Sci.* 2018;1418(1):44-55.

717   32.   Goujon JM, et al. Histological evaluation of proximal tubule cell injury in isolated
718   perfused pig kidneys exposed to cold ischemia. *J Surg Res.* 1999;82(2):228-33.

719   33.   Tirapelli LF, et al. Comparison of two models for evaluation histopathology of
720   experimental renal ischemia. *Transplant Proc.* 2009;41(10):4083-7.

721   34.   Havasi A, and Borkan SC. Apoptosis and acute kidney injury. *Kidney Int.*
722   2011;80(1):29-40.

723   35.   Daemen MA, et al. Inhibition of apoptosis induced by ischemia-reperfusion prevents
724   inflammation. *J Clin Invest.* 1999;104(5):541-9.

725   36.   Mellis AT, et al. The role of glutamate oxaloacetate transaminases in sulfite
726   biosynthesis and H(2)S metabolism. *Redox Biol.* 2021;38:101800.

727   37.   Kumar A, et al. S-sulfocysteine/NMDA receptor-dependent signaling underlies
728   neurodegeneration in molybdenum cofactor deficiency. *J Clin Invest.*
729   2017;127(12):4365-78.

730   38.   Grundmann F, et al. Dietary restriction for prevention of contrast-induced acute kidney
731   injury in patients undergoing percutaneous coronary angiography: a randomized
732   controlled trial. *Sci Rep.* 2020;10(1):5202.

733   39.   Yu D, et al. Short-term methionine deprivation improves metabolic health via sexually
734   dimorphic, mTORC1-independent mechanisms. *Faseb j.* 2018;32(6):3471-82.

735   40.   Solon-Biet SM, et al. Branched chain amino acids impact health and lifespan indirectly
736   via amino acid balance and appetite control. *Nat Metab.* 2019;1(5):532-45.

737   41.   Lieberthal W, et al. Rapamycin impairs recovery from acute renal failure: role of cell-
738   cycle arrest and apoptosis of tubular cells. *Am J Physiol Renal Physiol.*
739   2001;281(4):F693-706.

740   42.   Schwarz G. Molybdenum cofactor and human disease. *Curr Opin Chem Biol.*
741   2016;31:179-87.

742   43.   Kimura Y, et al. Sulfite protects neurons from oxidative stress. *Br J Pharmacol.*
743   2019;176(4):571-82.

744   44.   Kohl JB, et al. Homeostatic impact of sulfite and hydrogen sulfide on cysteine
745   catabolism. *Br J Pharmacol.* 2019;176(4):554-70.

746   45.   Filipovic MR, et al. Chemical Biology of H(2)S Signaling through Persulfidation.
747   *Chem Rev.* 2018;118(3):1253-337.

748   46.   Zivanovic J, et al. Selective Persulfide Detection Reveals Evolutionarily Conserved
749   Antiaging Effects of S-Sulfhydration. *Cell Metab.* 2019;30(6):1152-70.e13.

750   47.   Ruckenstuhl C, et al. Lifespan extension by methionine restriction requires autophagy-
751   dependent vacuolar acidification. *PLoS Genet.* 2014;10(5):e1004347.

752   48.   Jiang M, et al. Autophagy in proximal tubules protects against acute kidney injury.
753   *Kidney Int.* 2012;82(12):1271-83.

754   49.   Jiang M, et al. Autophagy is a renoprotective mechanism during in vitro hypoxia and
755   in vivo ischemia-reperfusion injury. *Am J Pathol.* 2010;176(3):1181-92.

756   50.   Ramos-Lopez O, et al. DNA methylation signatures at endoplasmic reticulum stress
757   genes are associated with adiposity and insulin resistance. *Mol Genet Metab.*
758   2018;123(1):50-8.

759   51.   Mangali S, et al. Inhibition of protein kinase R protects against palmitic acid-induced
760   inflammation, oxidative stress, and apoptosis through the JNK/NF-kB/NLRP3 pathway
761   in cultured H9C2 cardiomyocytes. *J Cell Biochem.* 2019;120(3):3651-63.

762   52.   Lynch EM, and Kollman JM. Coupled structural transitions enable highly cooperative
763   regulation of human CTPS2 filaments. *Nat Struct Mol Biol.* 2020;27(1):42-8.

764   53.   Aufhauser DD, Jr., et al. Improved renal ischemia tolerance in females influences
765   kidney transplantation outcomes. *J Clin Invest.* 2016;126(5):1968-77.

766   54.   Powell CR, et al. A review of hydrogen sulfide (H(2)S) donors: Chemistry and potential
767   therapeutic applications. *Biochem Pharmacol.* 2018;149:110-23.

768   55.   Jakubiczka-Smorag J, et al. Mouse model for molybdenum cofactor deficiency type B
769   recapitulates the phenotype observed in molybdenum cofactor deficient patients. *Hum*
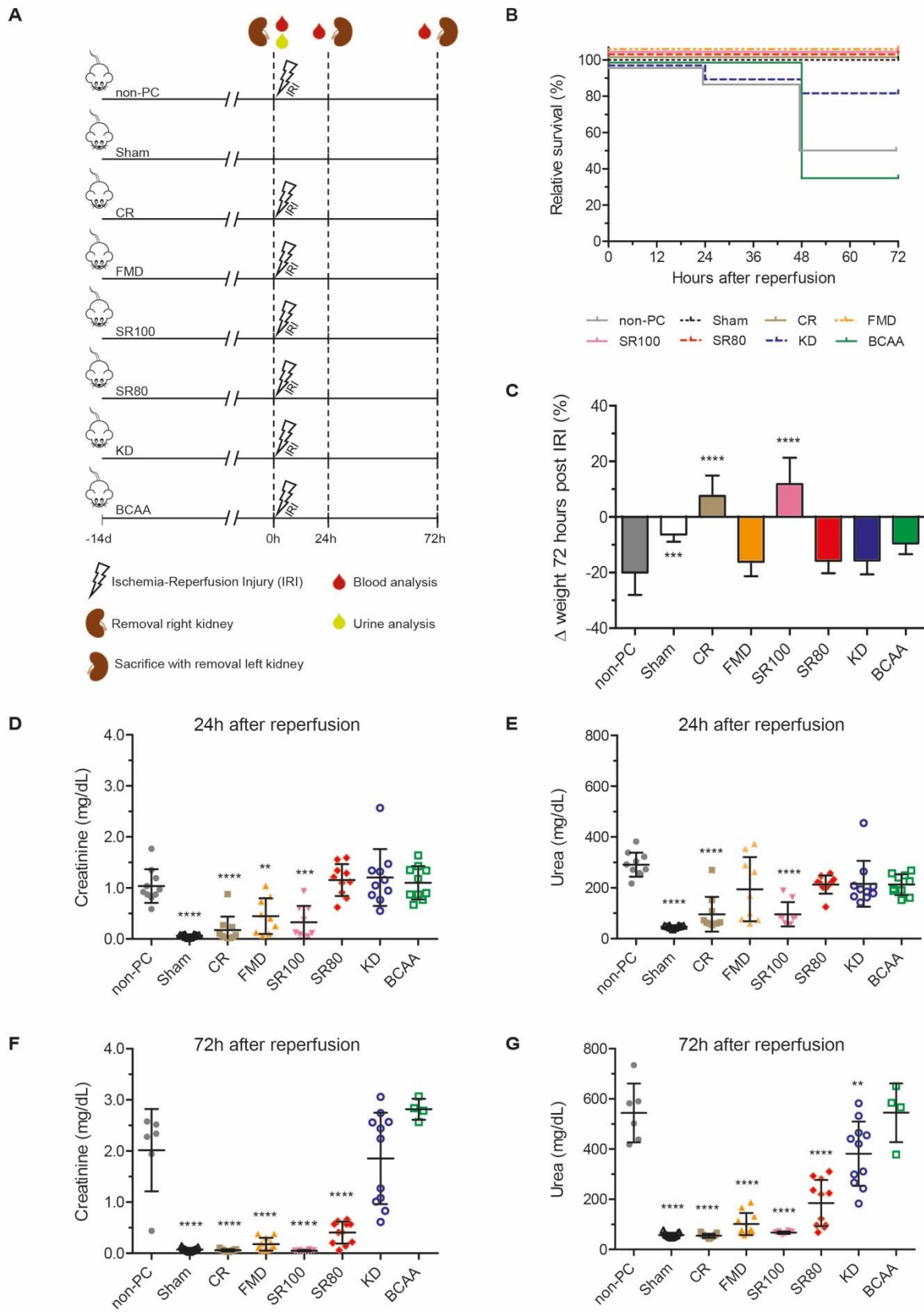770   *Genet.* 2016;135(7):813-26.

771

Figures

774 **Fig. 1. Direct comparison of different tailored dietary interventions identifies FMD and**

775 **SR80/100 as potent approaches protecting from renal IRI beyond CR.**

776 **(A)** Schematic of the experimental design depicting dietary preconditioning modes. CR served

777 as positive control, non-PC as negative. Sham animals underwent right nephrectomy without

778 clamping of the left renal pedicle and do not develop acute kidney injury. **(B)** Survival curves

779 of dietary preconditioned, non-preconditioned and sham animals after renal IRI. FMD, KD and

780 both low-SAA diets SR80/100 led to a significant survival advantage. **(C)** Delta body weight

781 of dietary preconditioned, non-preconditioned and sham animals 72 hours after reperfusion or

782 surgery, respectively, compared to the respective animal before IRI. Data are represented as

783 mean ± standard deviation. **(D, E)** Creatinine and urea concentrations 24 hours after

784 reperfusion or surgery, respectively. **(F, G)** Creatinine and urea concentrations 72 hours after

785 reperfusion or surgery, respectively. Kaplan Meier Analysis (log rank test *****P < 0.0001*, n

786 = 13 per group) was used in (A), One-way ANOVA and Bonferroni multiple comparison test

787 across all dietary preconditioning groups indicating differences to non-PC mice (***P < 0.01*,

788 ****P < 0.001* and *****P < 0.0001*) was used in (C)-(G) Data are represented as mean ±

789 standard deviation in (C)-(G) and each mice is depicted by a single dot. Abbreviations: BCAA:

790 Dietary Restriction of Branched Chain Amino Acids; CR: Caloric Restriction; d: day; FMD:

791 Fasting Mimicking Diet; h: hour; IRI: Ischemia-Reperfusion Injury; KD: Ketogenic Diet; non-

792 PC: non-preconditioned animals; SR100: 100% Restriction of Sulfur-containing Amino Acids;
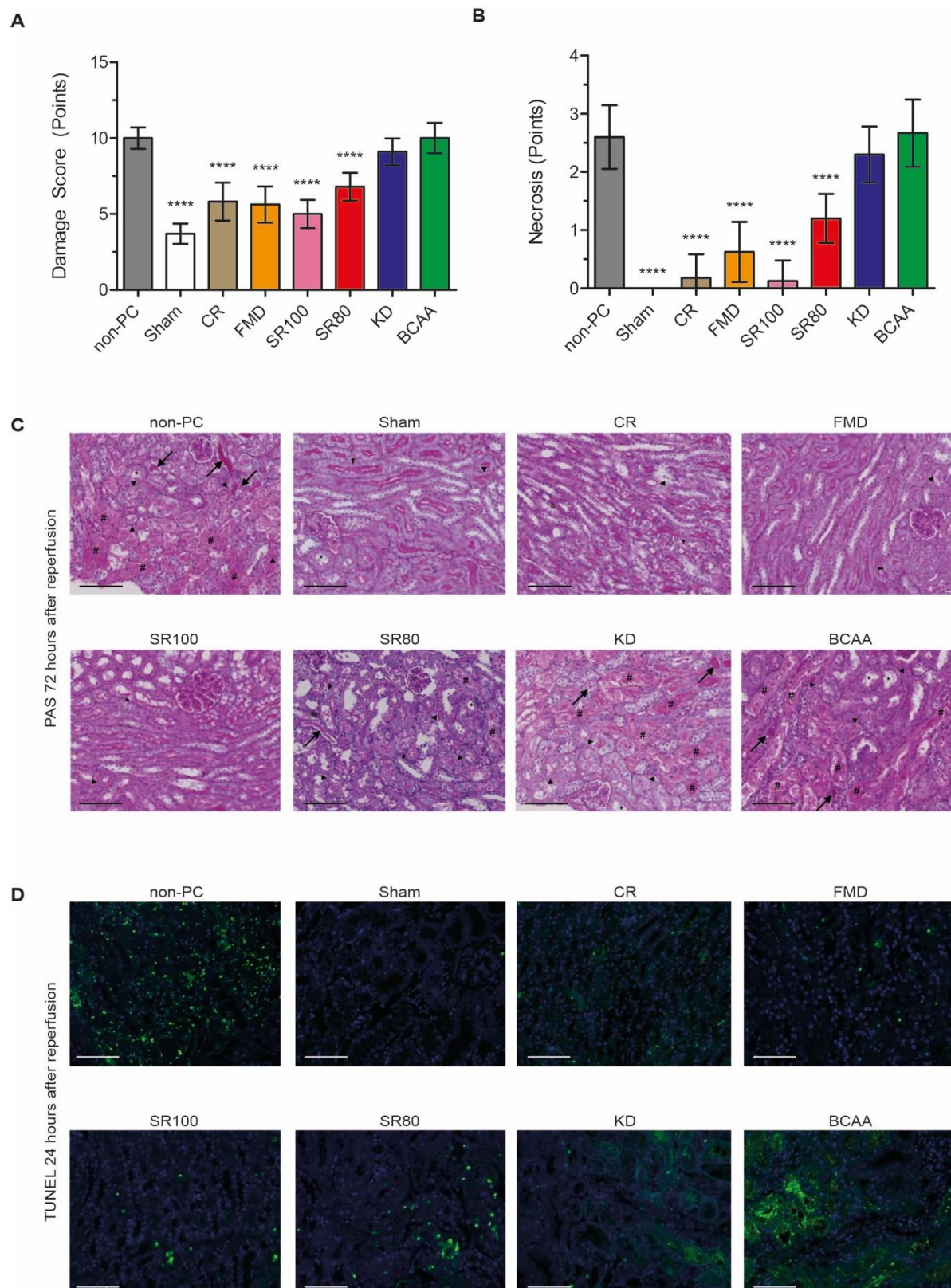
793 SR80: 80% Reduction of Sulfur-containing Amino Acids.

794

Fig. 2. Dietary preconditioning by FMD, SR80/100 and CR efficiently prevent tissue damage and cell death after renal IRI.

798 **(A, B)** Histologic damage and necrosis score at 72 hours after reperfusion examined in dietary

799 preconditioned, non-preconditioned and sham animals. One-way ANOVA and Bonferroni

800 multiple comparison test across all dietary preconditioning groups indicating differences to

801 non-PC mice (*****$P < 0.0001$*). Data are represented as mean ± standard deviation. 24h after

802 IRI: n = 10 per group; 72h after IRI n = 13 in the FMD, SR80/100, CR and sham group, n = 9

803 in the KD, n = 4 in the BCAA and n = 6 in the non-PC group, respectively. hours after

804 reperfusion Arrowheads indicate nuclei loss, arrows tubular casts, * epithelial flattening and #

805 denuded tubuli with luminar debris, respectively.Terminal deoxynucleotidyl transferase–

806 mediated digoxigenin-deoxyuridine nick-end labeling (TUNEL) assay at 24 hours after

807 reperfusion from dietary preconditioned, non-preconditioned and sham animals. Cell death in

808 green . Abbreviations: BCAA: Dietary Restriction of Branched Chain Amino Acids; CR:

809 Caloric Restriction; FMD: Fasting Mimicking Diet; KD: Ketogenic Diet; non-PC:

810 non-preconditioned animals; PAS: SR100: 100% Restriction of Sulfur-containing Amino

811 Acids; SR80: 80% Reduction of Sulfur-containing Amino Acids; TUNEL: Terminal

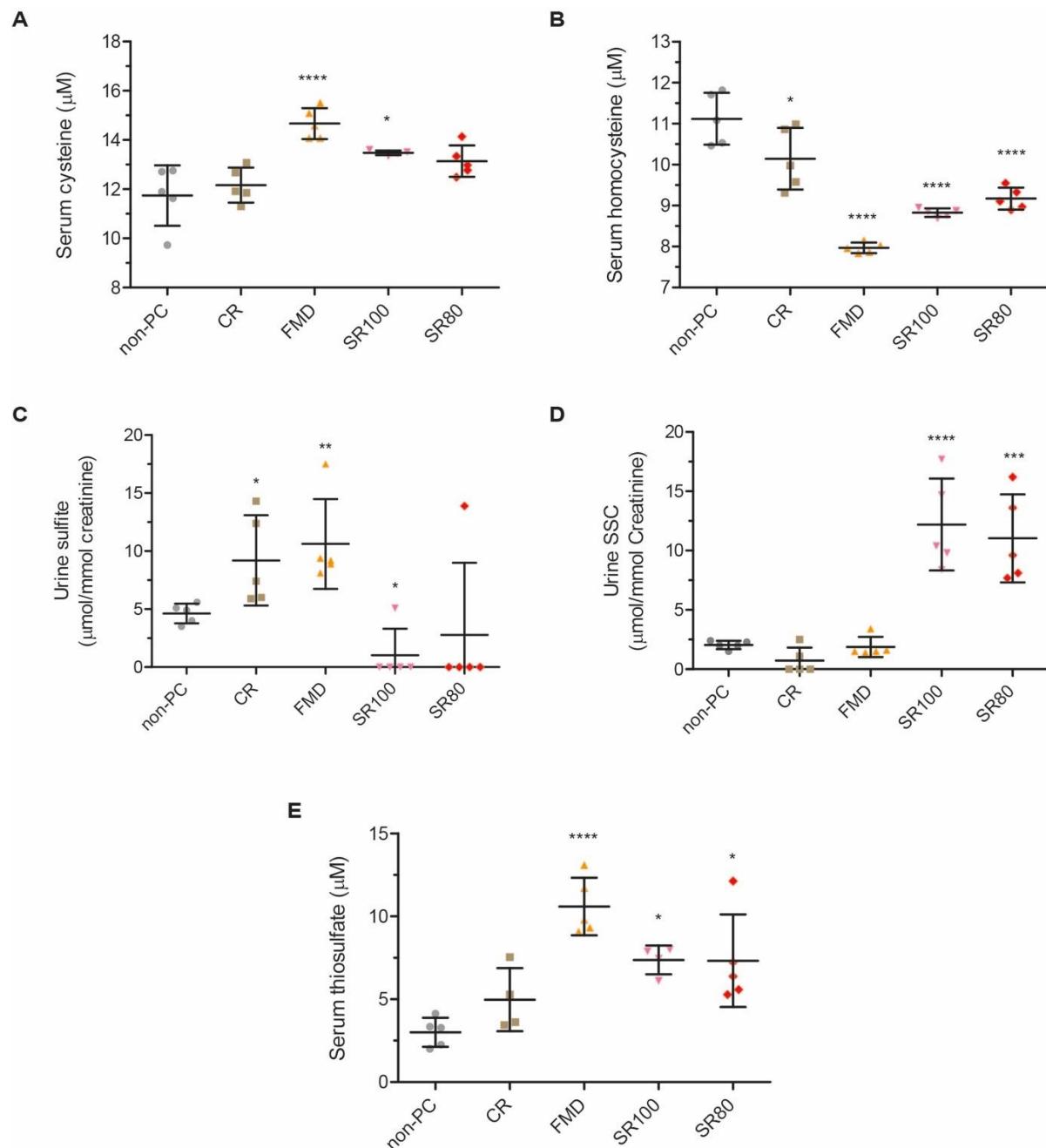812 deoxynucleotidyl transferase–mediated digoxigenin-deoxyuridine nick-end labeling.

813

814

Fig. 3. FMD, SR80/100 and CR modulate the oxidative and hydrogen sulfide dependent cysteine catabolism with sulfite as key intermediate.

(**A, B**) Serum cysteine and homocysteine values measured in dietary preconditioned and non-preconditioned mice at baseline. (**C**) Urine sulfite values measured in dietary preconditioned and non-preconditioned mice at baseline. (**D**) Urine s-sulfocysteine (SSC) values measured in dietary preconditioned and non-preconditioned mice at baseline. (**E**) Serum thiosulfate values measured in dietary preconditioned and non-preconditioned mice at baseline. One-way

38

822   ANOVA and Bonferroni multiple comparison test across all dietary preconditioning groups

823   indicating differences to non-PC mice (*P <0.05, **P < 0.01, ***P < 0.001 and

824   ****P < 0.0001) was used in (A), (B), (D) and (E). Unpaired T-test between dietary

825   preconditioned and non-preconditioned mice (*P < 0.05 and **P < 0.01) was used in (C). All

826   data are represented as mean ± standard deviation and each mice is depicted by a single dot.

827   Abbreviations: CR: Caloric Restriction, FMD: Fasting Mimicking Diet; non-PC:

828   non-preconditioned mice; SR100: 100% Restriction of Sulfur-containing Amino Acids; SR80:

829   80% Reduction of Sulfur-containing Amino Acids, SSC: S-sulfocysteine.

830

Fig. 4. Key enzymes in cysteine catabolism are differentially regulated in response to FMD and SR100.

Cysteine is either imported or generated from methionine and cysteine is either degraded to glutathione or taurine, or it is metabolized via the oxidative or the hydrogen sulfide (H_2S)-dependent branches to sulfate, thiosulfate and s-sulfocysteine (SSC), respectively. Sulfite is the major intermediate in both oxidative and H_2S-dependent cysteine catabolism. Enzymes significantly regulated *(p<0.05, log2FC > 0.6 or < -0.6)* after FMD or SR100 are assigned by colored arrows (Fasting Mimicking Diet (FMD): orange; 100% Restriction of Sulfur-

840   containing Amino Acids (SR100): pink). Enzymes are depicted as ellipsis. Arrows with solid

841   line indicate enzymatic, arrows with dashed lines non-enzymatic reactions, respectively. The

842   investigated major end-products of the H_2S-generating branch SSC and thiosulfate are written

843   in bold. Abbreviation: IMS: mitochondrial intermembrane space; SSC: S-sulfocysteine.
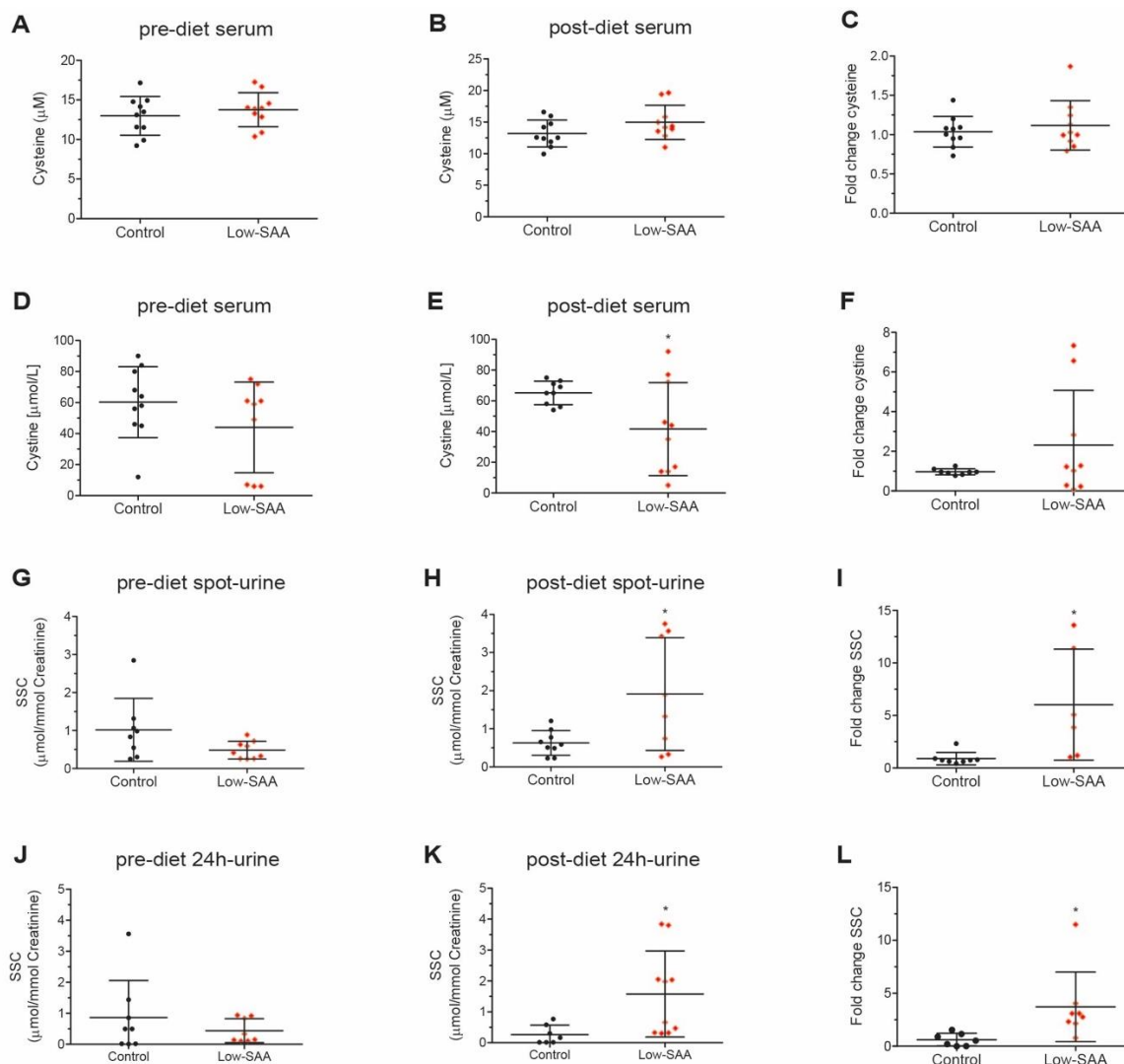
844

845

Fig. 5. Metabolic changes in oxidative and hydrogen sulfide (H₂S)-dependent cysteine catabolism are induced by short-term dietary preconditioning with low-SAA in humans. (**A ,B**) Cysteine concentrations measured in human serum samples after 7 days of control or low-SAA diet, before and after dietary intervention. (**C**) Individual fold change of cysteine levels in serum of the control and low-SAA groups. (**D, E**) Cystine concentrations measured in human serum samples after 7 days of control or low-SAA diet, before and after dietary intervention. (**F**) Individual fold change of serum cystine levels in the control and low-SAA groups. (**G, H**) S-sulfocysteine (SSC) concentrations measured in human spontaneous urine (spot-urine) samples after 7 days of control or low-SAA diet, before and after dietary intervention. (**I**) Individual fold change of SSC levels in spot-urine in the control and low-SAA

856   groups. **(J, K)** SSC concentrations measured in 24h collected human urine samples after 7 days

857   of control or low-SAA diet, before and after dietary intervention. **(L)** Individual fold change of

858   SSC levels in 24h collected urine samples in the control and low-SAA groups. Unpaired T-test

859   of low-SAA compared to control diet (*P < 0.05*) was used in (A)-(L). All data are represented

860   as mean ± standard deviation and each participant is depicted by a single dot. Abbreviations:

861   h: hour; SAA: Sulfur-containing Amino Acids; spot-urine: spontaneous urine; SSC:
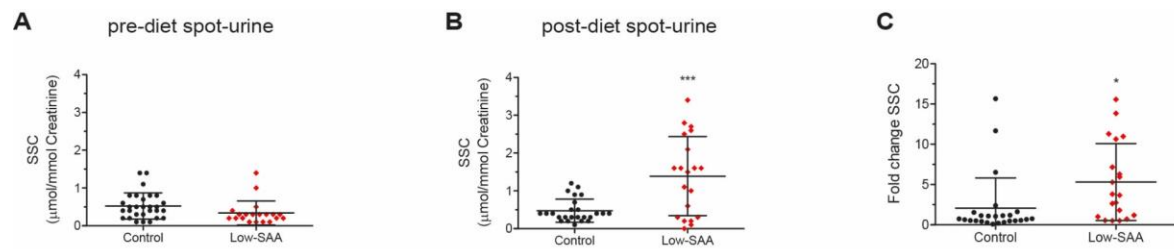
862   S-sulfocysteine.

863

864

Fig. 6. S-sulfocysteine – a key end-product of the H$_2$S generating branch of cysteine catabolism – is induced upon a low-SAA diet in humans.

(A, B) S-sulfocysteine (SSC) concentrations measured in spontaneous urine (spot-urine) samples of patients before and after the dietary intervention (control (N=29) and low-SAA (N=20)). **(C)** Individual fold change of SSC levels in spot-urine of after control or low-SAA diet. Unpaired T-test of low-SAA compared to control arm (*$P < 0.05$*) was used in (A)-(C). All data are represented as mean ± standard deviation and each patient is depicted by a single dot. Abbreviations: h: hour; SAA: Sulfur-containing Amino Acids; spot-urine: spontaneous urine; SSC: S-sulfocysteine.

874